Biophysical Chemistry 140 (2009) 78–90

Contents lists available at ScienceDirect

Biophysical Chemistry

journal homepage: http://www.elsevier.com/locate/biophyschem

# Interaction of the adenoviral IVa2 protein with a truncated viral DNA packaging sequence

Teng-Chieh Yang, Qin Yang, Nasib Karl Maluf *

*University of Colorado Denver, Department of Pharmaceutical Sciences, School of Pharmacy C238-P15, P.O Box 6511, Aurora, CO, 80045, United States*

ARTICLE INFO

*Article history:*
Received 26 September 2008
Received in revised form 25 November 2008
Accepted 25 November 2008
Available online 7 December 2008

*Keywords:*
IVa2
Viral DNA packaging
Analytical ultracentrifugation
Protein DNA interactions
Sequence specific DNA binding
Adenovirus

ABSTRACT

Adenoviral (Ad) infection typically poses little health risk for immunosufficient individuals. However, for immunocompromised individuals, such as AIDS patients and organ transplant recipients, especially pediatric heart transplant recipients, Ad infection is common and can be lethal. Ad DNA packaging is the process whereby the Ad genome becomes encapsulated by the viral capsid. Specific packaging is dependent upon the packaging sequence (PS), which is composed of seven repeated elements called A repeats. The Ad protein, IVa2, which is required for viral DNA packaging, has been shown to bind specifically to synthetic DNA probes containing A repeats I and II, however, the molecular details of this interaction have not been investigated. In this work we have studied the binding of a truncated form of the IVa2 protein, that has previously been shown to be sufficient for virus viability, to a DNA probe containing A repeats I and II. We find that the IVa2 protein exists as a monomer in solution, and that a single IVa2 monomer binds to this DNA with high affinity ($K_d$ < ~ 10 nM), and moderate specificity, and that the trIVa2 protein interacts in a fundamentally different way with DNA containing A repeats than it does with non-specific DNA. We also find that at elevated IVa2 concentrations, additional binding, beyond the singly ligated complex, is observed. When this reaction is modeled as representing the binding of a second IVa2 monomer to the singly ligated complex, the $K_d$ is 1.4±0.7 μM, implying a large degree of negative cooperativity exists for placing two IVa2 monomers on a DNA with adjacent A repeats.

Published by Elsevier B.V.

## 1. Introduction

Human adenovirus (Ad) can cause infections of the respiratory tract, urinary tract, and gastrointestinal tract, among others [1], and acute respiratory infections are common in young children and military recruits [2–4]. Recently, a reemergence of the Ad serotype 14, previously identified in 1955, has been linked to severe acute respiratory disease [2,4], although other Ad serotypes typically pose little health risk to immunosufficient individuals. However, for individuals with compromised immune systems, such as AIDS patients and organ transplant recipients, especially pediatric heart transplant recipients, adenoviral infection is common and can be lethal [1,3,5,6].

The human adenovirus type 5 (Ad5) genome is approximately 36 kb, and is condensed inside an icosahedral capsid [7]. The genome is bound by approximately 1200 copies of the viral histone-like VII protein, which serve to condense the genome inside the capsid [8]. Additional viral proteins are found within the capsid [7,9]: the terminal protein is covalently attached to the 5′ ends of the genome, and serves to prime DNA replication. Protein V appears to interact simultaneously with the interior of the capsid and the genome. Finally, peptide mu binds to and helps condense the viral genome.

The mechanism of viral DNA packaging in Ad is controversial. It has long been presumed that adenoviral DNA packaging proceeds similarly to its distant relative, the bacteriophage [9]. In this model, the viral DNA is packaged into a preformed capsid through a specialized vertex which serves as the entry point for the DNA [10,11]. By analogy with bacteriophages, a motor protein presumably is required to translocate the DNA into the capsid. Evidence for this model is as follows. First, early pulse-chase experiments showed that radiolabeled amino acids incorporated into incomplete capsids before they incorporated into mature virus particles, suggesting capsids form before the DNA is packaged [12]. Second, when certain temperature-sensitive adenovirus mutants (ts369 and ts112) were grown at the non-permissive temperature, incomplete virus particles were isolated that contained variable lengths of the left end of the viral genome [13,14]. This suggests packaging of the genome proceeds directionally, beginning at the left end of the genome. On the other hand, protein VII associates with the unpackaged viral DNA during the late phase of Ad infection [15–18]. This result seems difficult to reconcile with the idea the DNA could be translocated into a preformed capsid [19]. One possibility is a novel mechanism which would involve directionally packaging the condensed DNA into the preformed capsid [19]; in this case the presumed DNA packaging machinery would have to

* Corresponding author. Tel.: +1 303 724 4036; fax: +1 303 315 6285.
*E-mail address:* karl.maluf@uchsc.edu (N.K. Maluf).

0301-4622/$ – see front matter. Published by Elsevier B.V.
doi:10.1016/j.bpc.2008.11.014

accommodate the bound VII protein during the packaging process. A simpler model is that the capsid assembles around the condensed DNA, similar to the model for packaging of the RNA genome of the poliovirus [19–22]. Along these lines, a possible explanation for the pulse-chase experiments is that capsid assembly is reversible, so that assembled, empty capsids may dissociate then reassemble around the condensed DNA [23].

The Ad IVa2 protein was first identified as a transcriptional activator of the major late promoter (MLP) [24]. IVa2, which was purified from Ad infected cells, was shown to bind specifically to an element downstream from the transcriptional start site (DE element), using electrophoretic mobility gel-shift assays (EMSA) [24]. UV-induced crosslinking studies as well as glycerol-gradient sedimentation studies were interpreted to suggest IVa2 bound to the DE element as a dimer [25], and additional glycerol gradient studies suggested IVa2 existed as a monomer in the absence of DNA [25]. Further EMSA experiments also identified an additional 'infected cell specific' protein which correlated with activation of transcription from the MLP [24,25]. Recent experiments have identified this factor to be the viral L4-33 kDa protein, and suggest IVa2 and L4-33 kDa interact with each other, since they can be co-purified by two different procedures [26].

More recently, IVa2 has been shown to be required for both capsid assembly and viral DNA packaging [23,27,28]. A IVa2 mutant was designed that contained two stop codons, at aa positions 17 and 19 in the primary structure [23]. While this mutant virus could still replicate its DNA and produce early and late viral genes, infectious virus was not produced. Electron microscopy (EM) did not detect any viral particles in transfected cells, indicating capsid assembly did not occur. The mutant could be rescued if transfected into cells that constitutively express cloned wt IVa2, or if cotransfected with the wt IVa2 gene. Interestingly, if IVa2 levels were decreased ~20 fold, while the mutant could still be rescued, viral yield was decreased ~100 fold, and many abnormally shaped (i.e. non-icosahedral) viral particles were observed by EM [23], suggesting IVa2 plays a role in the proper assembly of the viral capsid.

IVa2 has been shown to bind specifically to the PS located at the left end of the viral genome [27–31]. This sequence contains seven repeated elements called A repeats, due to their A–T rich nature, and is required for DNA packaging (Fig. 1). While the A repeats are functionally redundant, it has been shown that some are more effective than others for signaling viral assembly, with a hierarchy of importance of AI, AII, AV, and AVI, based on genetic experiments [9,32,33]. Consequently, DNA probes containing these repeats, especially repeats I and II, have been used to investigate specific binding of IVa2 to DNA [28–31,34,35].

A consensus motif for the A repeat sequence has been reported as 5′-TTTG-$N_8$-CG-3′ [33]. Fig. 1 shows that several of the A repeat pairs are also arranged so that the CG motif of an upstream A repeat is spaced seven bp from the TTTG motif of an adjacent, downstream A repeat. For example, see A repeats I and II in Fig. 1. Fig. 1 also shows that the DE element contains a TTTG and CG motif, and these two motifs are arranged as 5′-CG-$N_7$-TTTG-3′, which is the same spacing (discussed above) seen between several pairs of A repeats.

EMSA experiments performed with a DNA probe possessing A repeats I and II (A-I-II), using extracts derived from Ad-infected human cells, show up to three viral-specific protein–DNA bands [27,29–31,34]. All of these bands have been shown to possess IVa2 by multiple methods, including western analysis. Mutational analysis, both in vivo and in vitro, indicates the CG element of the consensus motif, and *not* the TTTG motif, is required for specific IVa2 binding [27,29–31,34].

Mutational analysis of the TTTG element present within the A repeats, indicates an additional viral specific protein, recently identified as the L4-22K protein, is responsible for binding to this element [29,34]. The L4-22K protein is translated from the same transcript that produces the L4-33 kDa protein, except that the L4-33 kDa protein is translated from a spliced version of this transcript; the L4-22K protein is translated from the unspliced version of the transcript. These proteins share the first 105 aa's, but have different C-termini (124 aa's for L4-33 kDa, and 91 aa's for L4-22K). Recent experiments suggest the L4-33K protein interacts with the TTTG motif present within the DE element to stimulate transcription from the major late promoter [26].

Recent genetic experiments have shown that the L4-22K protein plays a critical role in DNA packaging [34,36,37]. When certain amber mutants were introduced into the L4-22K gene, either the mutation was lethal or virus production was reduced. Furthermore, these mutant viruses replicated and expressed the late viral gene products; thus the phenotype was not simply due to a loss of DNA replication or gene expression. EMSA experiments, performed with proteins derived from cell extracts, suggested the L4-22K protein required IVa2 to bind to the TTTG motif of the A sequences [34], and this result has been reproduced with purified recombinant IVa2 and L4-22K [29,30]. Recent EMSA experiments show the presence of the purified L4-22K protein increases the apparent affinity of the IVa2 protein for the PS DNA, strongly suggesting heterotropic cooperative interactions occur between IVa2 and L4-22K that might play a role in controlling the onset of viral DNA packaging [29]. In addition to these results, recent

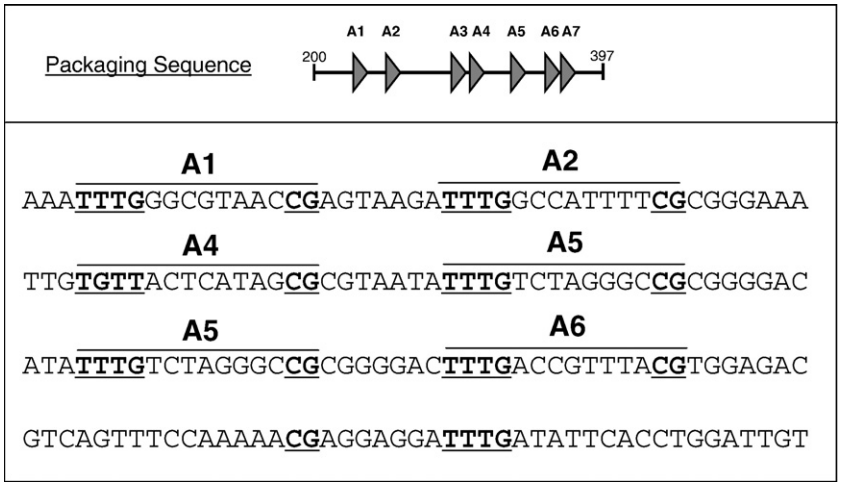


**Fig. 1.** The top panel shows a schematic of the packaging sequence, located between bp 200 and 397 of the human Ad (type 5) genome. The bottom panel shows an alignment of some of the A repeats with the DE element. The TTTG and CG motifs previously identified have been shown. Previous EMSA data collected using cell extracts predict the T and G switch observed in the A4 repeat will affect L4-22K binding at this particular position [6]. This figure is modified from Ostapchuk and Hearing [9].

experiments have shown a direct, protein–protein interaction between IVa2 and the L4-33K protein [26]; thus it is possible IVa2 and L4-22K also interact with each other, and that this interaction motif is present within the first 105 aa residues of the L4-22K protein. If so, this interaction may facilitate cooperative binding of both proteins on the PS DNA.

To begin to understand how the IVa2 protein recognizes the PS DNA, we have studied the binding of a truncated form of the IVa2 protein to a truncated PS DNA molecule, using rigorous sedimentation equilibrium and velocity methods.

## 2. Materials and methods

### 2.1. Sample preparation

The trIVa2 gene was cloned into pKKT7 [38] and transformed into *E. coli* BL21(DE3). The cells were grown in a shaker in 1L LB at 37 °C to an OD of 0.6. Expression of trIVa2 was induced by addition of 0.5 mM IPTG, followed by incubation with shaking at 37 °C for an additional 4 h, and harvested by centrifugation. All purification steps were performed at 4 °C. The cells were resuspended with 10 mL lysis buffer (100 mM NaCl, 50 mM Tris, pH 8.65 at 4 °C, 10 mM EDTA, 10 mM β-me and 10%(v/v) glycerol), and lysed with 0.4 mg/mL lysozyme (from Roche) for 30 min followed by sonication. The lysed cells were centrifuged at 17,000 ×g for 30 min. The vast majority of expressed trIVa2 was found in the cell pellet. The cell pellet was resuspended with 10 mL of 6 M Guanidine HCL+40 mM HEPES, 1 mM EDTA and 10 mM β-me, diluted to 1 L with the same buffer, then dialyzed against 3 changes (3 L each) of refolding buffer (150 mM NaCl, 40 mM HEPES, pH 7.6, 1 mM EDTA, 10 mM β-me and 10%(v/v) glycerol). Each change was allowed to dialyze for at least 6 h. The dialyzed solution was cleared by centrifugation, then subjected to SP sepharose chromatography (HI trap SP column, 5 mL from Pharmacia). The column was washed with 5 column volumes of refolding buffer, then the protein was eluted with refolding buffer+1 M NaCl. The eluted protein was brought up to 1 M $(NH_4)_3SO_4$ by slow addition of refolding buffer containing 3 M $(NH_4)_3SO_4$ and 1 M NaCl. Next, the protein was loaded onto a 5 mL HiTrap Butyl-S Sepharose hydrophobic column, washed with 5 column volumes of refolding buffer+1 M $(NH_4)_3SO_4$+1 M NaCl, then washed with 4 column volumes of refolding buffer+850 mM $(NH_4)_3SO_4$+375 mM NaCl. The protein was eluted with refolding buffer+50 mM NaCl. The purified protein was dialyzed into storage buffer (500 mM NaCl, 50%(v/v) glycerol, 40 mM HEPES, pH 7.6, 1 mM EDTA, and 10 mM β-me), flash frozen with liquid nitrogen and stored frozen long-term at −80 °C. Thawed samples were then stored short-term (up to 2 months) at −20 °C. Protein purified by this procedure was greater than 99% pure as judged by SDS-page electrophoresis followed by Commassie staining. The protein concentration was determined by absorbance spectroscopy, using an extinction coefficient of 0.0469 $\mu M^{-1}cm^{-1}$, calculated using the method of Gill and von Hippel [39]. This procedure produces ~1 mg pure trIVa2 per liter of cell culture.

DNA molecules were purchased from IDT (Iowa City, IA), and were purified by HPLC. The top strand of the ds A-I-II-Cy3 DNA used in this study has the following sequence: 5′-Cy3-TAGTAAATTTGGGCGTAACC-GAGTAAGATTTGGCCATTTTCGCGGGAA-3′. The DNA concentrations were determined by absorbance spectroscopy using the calculated extinction coefficient at 260 nm based on the nearest neighbor method [40]. The extinction coefficient at 522 nm for the Cy3 dye was measured using absorbance spectroscopy, and was determined to be 0.0869 $\mu M^{-1}cm^{-1}$, using a value of 0.1325 $\mu M^{-1}cm^{-1}$ for the extinction coefficient at 550 nm [41]. The DNA was annealed by mixing a slight excess (1.25 fold) of the bottom, unlabeled DNA with the top strand in Buffer H, boiling for 5 min, then cooling at room temperature for 30 min. The unlabeled DNAs were annealed by mixing the top and bottom strands at a 1:1 molar ratio, boiling for 5 min, then cooling at room temperature for 30 min. Sedimentation velocity experiments confirmed 100% annealing of the Cy3-labled DNA molecules, and greater than 94% annealing for the unlabeled DNA molecules. Control experiments demonstrated that 100 nM single stranded 48-mer DNA (to mimic a slight excess of one strand to the other) did not compete, at a detectable level, with the binding of the trIVa2 protein with the ds DNA.

### 2.2. Sedimentation velocity experiments

Sedimentation velocity experiments were performed using a Beckman XLA ultracentrifuge. Purified protein was dialyzed into Buffer H (100 mM NaCl, 40 mM HEPES, pH 7.6 at 25 °C, 10%(v/v) glycerol, and 1 mM TCEP). For experiments performed on the free trIVa2 protein, data were collected at 280 nm, every 0.003 cm with 2 averages in the continuous scan mode. Protein samples (300 or 400 μL) were loaded into Epon aluminum-filled 2 sector centerpieces, and experiments were performed at 25 °C, at 50K RPM. At least 1.5 h were allowed for temperature equilibration of the samples and instrument prior to the start of the experiment. The binding of trIVa2 to the Cy3-labled DNA molecules was examined at 522 nm, due to increased lamp intensity at 522 nm when compared to the lamp intensity at 550 nm. The protein and DNA samples were dialyzed into Buffer H, then mixed at the appropriate concentrations. The raw sedimentation velocity data was analyzed using the SEDFIT and SEDPHAT programs [42], and the sedimentation coefficients were corrected to standard conditions (20 °C, in $H_2O$) using SEDFIT. The $s_{20,w}$ values reported for the A-I-II-Cy3 DNA molecule, and for the 1:1 trIVa2:A-I-II-Cy3 complexes did not include a temperature correction for the partial specific volume, since data for the temperature dependence of the partial specific volume of the DNA were not available [43]. The reported $s_{20,w}$ value for the trIVa2 protein did include this temperature correction, which was calculated using $\overline{\upsilon}_{20\ °C} = \overline{\upsilon}_{25\ °C} - 2.125\times10^{-3}$ [43].

### 2.3. Sedimentation equilibrium experiments

Protein and DNA samples were dialyzed into Buffer H. The samples (120 μL) were loaded into Epon aluminum filled 6 sector centerpieces, and sedimented to equilibrium at 25 °C, at the indicated rotor speed. Equilibrium was established well before 24 h at each speed, and was checked by overlaying successive scans. Data were collected every 0.001 cm, in the step-mode, with 20 averages/step. Experiments performed on the trIVa2 protein alone were preformed at 280 nm, while experiments performed on the trIVa2/A-I-II-Cy3 mixtures were carried out at 522 nm.

### 2.4. Analysis of sedimentation equilibrium data

The buoyant molecular weight of a macromolecule subjected to translational sedimentation in a centrifugal field is given by:

$$M_b = M(1-\overline{\upsilon}\rho)$$

where $M$ is the molecular weight of the macromolecule, in g/mol, $\overline{\upsilon}$ is the partial specific volume of the macromolecule in mL/g, and $\rho$ is the density of the buffer, in g/mL. To calculate the predicted buoyant molecular weight of a particular trIVa2:DNA ligation state, the weight-averaged, partial specific volume of the complex was calculated using:

$$\overline{\upsilon}_n = \frac{nM_{trIVa2}\overline{\upsilon}_{trIVa2} + M_{DNA}\overline{\upsilon}_{DNA}}{nM_{trIVa2} + M_{DNA}}$$

which assumes a significant volume change does not occur upon complex formation. In this equation, $n$ represents the number of trIVa2 protein monomers bound to the DNA molecule. $\overline{\upsilon}_{trIVa2}$ was calculated based on the amino acid sequence using the program

SEDNTERP, yielding a value of $\bar{v}_{trIVa2}$=0.7406 mL/g (at 25 °C). $\bar{v}_{DNA}$ was calculated experimentally using the sedimentation equilibrium technique (Buffer H, 25 °C), yielding a value of $\bar{v}_{DNA}$=0.5525 mL/g. Based on these values, we calculate $\bar{v}_1$=0.6630 mL/g, and $\bar{v}_2$=0.6917 mL/g. These values were then used to calculate the buoyant molecular weights of the indicated trIVa2:DNA stoichiometries, according to:

$$M_{b,n} = (nM_{trIVa2} + M_{DNA})(1-\bar{v}_n\rho)$$

where $M_{trIVa2}$=42,767 g/mol, $M_{DNA}$=30,039 g/mol (for the A-I-II-Cy3 double stranded DNA molecule used here). The calculated buoyant molecular weight corresponding to a single trIVa2 monomer bound to the A-I-II-Cy3 DNA, i.e. $n$=1, was 22.9 kDa. The buoyant molecular weight corresponding to two trIVa2 monomers bound to a single A-I-II-Cy3 DNA, i.e. $n$=2, was 33.0 kDa. The buffer density, $\rho$, was calculated using SEDNTERP, which yielded 1.03298 mL/g (which ignores the small concentration of the TCEP reducing agent).

The data in Fig. 4 were analyzed by non-linear least squares (NLLS) methods using Eq. (1) (see Supplementary data, section *S.1*):

$$A_T = \left(\frac{A_{0,0}(r_b-r_m)\sigma_0}{e^{\sigma_0\xi_b}/r_b-1/r_m}\right)e^{\sigma_0\xi} + \left(\frac{A_{0,1}(r_b-r_m)\sigma_1}{e^{\sigma_1\xi_b}/r_b-1/r_m}\right)e^{\sigma_1\xi} + \alpha \quad (1)$$

where $A_T$ is the total absorbance at a radial position $r$, $A_{0,0}$ is the total, loading absorbance of the free DNA, $A_{0,1}$ is the total, loading absorbance of protein–DNA species, $r_m$ is the position of the meniscus, $r_b$ is the position of the base of the cell, $\xi \equiv (r^2-r_m^2)/2$, $\xi_b \equiv (r_b^2-r_m^2)/2$, and $\alpha$ is the baseline offset. $\sigma_0$ and $\sigma_1$ are given by $M_{b,0}\,\omega^2/RT$ and $M_{b,1}\,\omega^2/RT$, respectively, where $\omega$ is the rotor speed, $R$ is the gas constant and $T$ is the absolute temperature. As described above, the buoyant molecular weights are calculated as a function of protein/DNA ligation state, and the subscript 0 refers to the free DNA (unligated) DNA molecule. The data presented in Fig. 8 were analyzed according to the method described in the Supplementary data, section *S.1*, using Equations S12–S14.

### 2.5. Analysis of competition experiments using the sedimentation velocity approach

The specificity with which the trIVa2 protein bound to the A-I-II DNA was measured using the sedimentation velocity approach by competition methods. The data presented in Fig. 9 were analyzed by NLLS according to Eq. (2):

$$[P_T] = \left(\frac{s_{wt}-s_D}{s_{PD}-s_D}\right)[D_T] + \frac{(s_{wt}-s_D)Q}{(s_{PD}-Qs_D)+s_{wt}(Q-1)}[C_T] \quad (2)$$

where $s_{wt}$ is the weight averaged sedimentation coefficient, $s_D$ is the sedimentation coefficient of the free A-I-II-Cy3 DNA, $s_{PD}$ is the sedimentation coefficient of the 1:1 trIVa2/A-I-II-Cy3 DNA complex, $[P_T]$ is the total trIVa2 protein concentration, $[C_T]$ is the total competitor DNA concentration, $[D_T]$ is the total A-I-II-Cy3 DNA concentration, and $Q$ is the ratio of the equilibrium association constant for competitor binding to the equilibrium association constant for A-I-II-Cy3 binding (see Supplementary data, section *S.2*) The analysis was performed by implicitly solving Eq. (2) for the dependent variable, $s_{wt}$, at known total trIVa2, A-I-II-Cy3 and competitor DNA concentrations, using the Scientist (Micromath) software. The total trIVa2 concentration was calculated by multiplying the loading concentration, 2 μM, by the measured activity of the preparation, which was 0.529 (see Fig. 6 and Section 3.2), which yields 1.06 μM active trIVa2. $s_D$ and $s_{PD}$ were fixed at their previously determined values of 2.68 and 3.67 S (not corrected to standard conditions), which were determined from the global fit to the raw sedimentation velocity data shown in Fig. 5.

### 2.6. Hydrodynamic calculations

The frictional coefficient ratio, $f/f_0$, was calculated using:

$$\frac{f}{f_0} = \left(\frac{M^2(1-\bar{v}\rho)^3}{162\pi^2(s_{20,w})^3\eta^3N_{av}^2(\bar{v}+\delta\bar{v}^0_{H2O}))}\right)^{1/3}$$

where $\eta$ is the viscosity of pure water at 20 °C, $N_{av}$ is Avogadro's number, $\rho$ is the density of pure water at 20 °C, $\bar{v}$ is the partial specific volume of the macromolecule at 20 °C, $\bar{v}^0_{H2O}$ is the partial specific volume of pure water at 20 °C, and $\delta$ is the macromolecular hydration, in grams of water bound per gram of macromolecule [44]. For the trIVa2 protein, $\delta$ was calculated based on its primary sequence, using SEDNTERP, according to the method of Kuntz [44], which yielded a value of 0.3789 g/g.

The predicted $s_{20,w}$ for an unfolded, random coil polypeptide chain was calculated using the following equation:

$$s_{20,w} = 0.296M^{0.457}$$

where $M$ (kDa) is the molecular weight of the polypeptide chain. This equation was calculated from data presented in Uversky [45] for the sedimentation of a series of different sized proteins in 6 M guanidine HCl.

The frictional coefficient of a rigid rod cylinder was calculated using equations 5 and B1 from Koenderink et al. [46]:

$$f_{cyl} = \frac{3\pi\eta L}{\ln(L/d)+0.3863}$$

which is a valid model for double stranded DNA molecules shorter than about 200 bp [47]. $L$ is the length of the rod while $d$ is the diameter. The length of the 48 bp, A-I-II-Cy3 DNA used here was calculated by multiplying the number of bp by 0.337 nm rise/bp [46]. The diameter, $d$, was adjusted until agreement was found between the experimentally determined frictional coefficient of the A-I-II-Cy3 DNA and the predicted frictional coefficient of the cylinder, $f_{cyl}$. This resulted in a "hydrodynamic" diameter for the A-I-II-Cy3 DNA of 2.25 ± 0.15 nm, very similar to the value determined for a series of short duplex DNA molecules, of 2.26±0.14 nm using the same approach [48].

To calculate the hydration of the DNA molecule, $\delta$, we used the calculated hydrodynamic diameter of the A-I-II-Cy3 DNA to estimate its hydrated volume, according to $V_{hyd} = \pi(d/2)^2L$. $\delta$ was then calculated according to [49]:

$$\delta = \left(\frac{V_{hyd}N_{av}}{M}-\bar{v}\right)\rho$$

where $M$ and $\bar{v}$ correspond to the molecular weight and partial specific volume of the A-I-II-Cy3 DNA, and $\rho$ is the density of pure water. This calculation returned a value of 0.74±0.17 g/g, which corresponds to 25±5 water molecules/bp of DNA. It should be emphasized this calculation results in a model dependent estimate of the hydration, and that the measured hydration value seems to depend on the technique used [50].

The hydration value for the 1:1 trIVa2/A-I-II-Cy3 DNA was estimated by calculation of a weight averaged value for the complex, according to:

$$\delta_{1:1} = \frac{M_{trIVa2}\delta_{trIVa2}+M_{DNA}\delta_{DNA}}{M_{trIVa2}+M_{DNA}}$$

which returned a value of 0.528 g/g. This value was used to calculate the frictional coefficient ratio of the 1:1 trIVa2/A-I-II-Cy3 complex.

### 2.7. Double-stranded DNA cellulose chromatography

Double stranded DNA cellulose material was kindly provided by Dr. Tim Lohman, (Washington University in St. Louis), and was prepared according to Litman [51]. The total amount of DNA crosslinked to the cellulose material was ~0.63 mg/mL of packed column material. This was determined as follows. A 300 µL bed volume of dsDNA-cellulose was incubated with 20 µg/mL DNaseI (in 50 mM Tris, pH 8, 10 mM $MgCl_2$) for 30 min at 37 °C, with frequent mixing by hand. The digested material was poured into a small column, and the flow-through was collected. The flow-through was extracted with phenol/chloroform, then the aqueous phase was brought to a final concentration of 0.3 M sodium acetate (by addition of 1/10 volume of 3 M sodium acetate, pH 5.2), and 10 µg of linear acrylimide was added to serve as a carrier. The digested DNA was then precipitated using ethanol. The precipitated DNA was resuspended in water, and the concentration of DNA was determined using absorbance spectroscopy.

## 3. Results

### 3.1. The trIVa2 protein exists as a monomer in solution

Previous genetic experiments have shown that a truncated from of the IVa2 protein can function in vivo to produce infectious adenoviral particles [28]. These authors showed that translation of the IVa2 protein can begin at Met 75, producing a 42.8 kDa protein, based on the amino acid sequence. We found that this truncated version of IVa2, hereafter referred to as trIVa2, was easily over expressed in *E. coli*. The full length IVa2 protein was not efficiently over expressed in the same system, however, purification of a recombinant, full length IVa2 has been reported [30]. All the expressed trIVa2 protein was found in the cell debris pellet, therefore we purified the protein from the cell debris pellet by denaturation–renaturation using guanidine–HCl. The refolded protein was further subjected to SP sepharose and Butyl-S sepharose chromatography, resulting in folded, pure trIVa2. Protein purity was judged to be greater than 99% based on SDS-page electrophoresis followed by Commassie staining (Fig. 2A). Folding of the protein was investigated by sedimentation velocity analysis, and also inferred since the refolded protein possessed high-affinity DNA binding activity. These results will be discussed in the following sections.

The quaternary structure of trIVa2 was assessed by sedimentation velocity and equilibrium experiments. Fig. 2B shows a sedimentation velocity experiment performed in Buffer H at 25 °C, at a loading concentration of trIVa2 of 3.4 µM (Buffer H is 100 mM NaCl, 40 mM HEPES, pH 7.6, 10%(v/v) glycerol and 1 mM TCEP). The raw data were analyzed using the SEDFIT [42] program, and the $c(s)$ distribution is shown. A single, sharp peak, was observed in the $c(s)$ distribution which indicates trIVa2 exists as a single oligomeric species under these solution conditions. From the peak of the $c(s)$ distribution, the $s_{20,w}$ value was calculated to be 2.88±0.02 S (average and standard deviation calculated from 5 separate experiments). Since the sample is homogenous, the molecular weight of the species can be estimated by converting the $c(s)$ distribution into the corresponding $c(M)$ distribution [42], which is shown in the inset. The peak molecular weight occurs at about 40 kDa, which is slightly smaller than the predicted molecular weight of 42.8 kDa, based on the amino acid sequence. Additional experiments performed as a function of trIVa2 loading concentrations (0.5 to 6.7 µM) showed identical results (not shown). For comparison, an unfolded, random coil polypeptide chain of 42.8 kDa is predicted to have an $s_{20,w}$ of 1.65 S (see Section 2.6), which is much lower than the measured value of 2.88±0.02 S, suggesting the denaturation-refolding purification procedure was successful.

To further study the size of the trIVa2 protein in solution, we performed a sedimentation equilibrium experiment, at loading concentrations of 0.75 and 2.5 µM trIVa2, and show the results from the 2.5 µM loading concentration in Fig. 2C. The data were analyzed according to a single ideal species model, which returned a molecular weight of 43±3 kDa, consistent with the predicted molecular weight of the trIVa2 monomer. Thus, from the sedimentation velocity and equilibrium experiments, we conclude the trIVa2 protein exists as a monomer for concentrations up to about 6.7 µM.

### 3.2. Stoichiometry of binding of trIVa2 to a DNA with A repeats I and II

To study the stoichiometry of binding of trIVa2 to PS DNA, we investigated the binding of the trIVa2 protein with a 48 bp synthetic DNA that contained A repeats I and II (hereafter referred to as A-I-II-Cy3; see Fig. 1), using sedimentation velocity and equilibrium

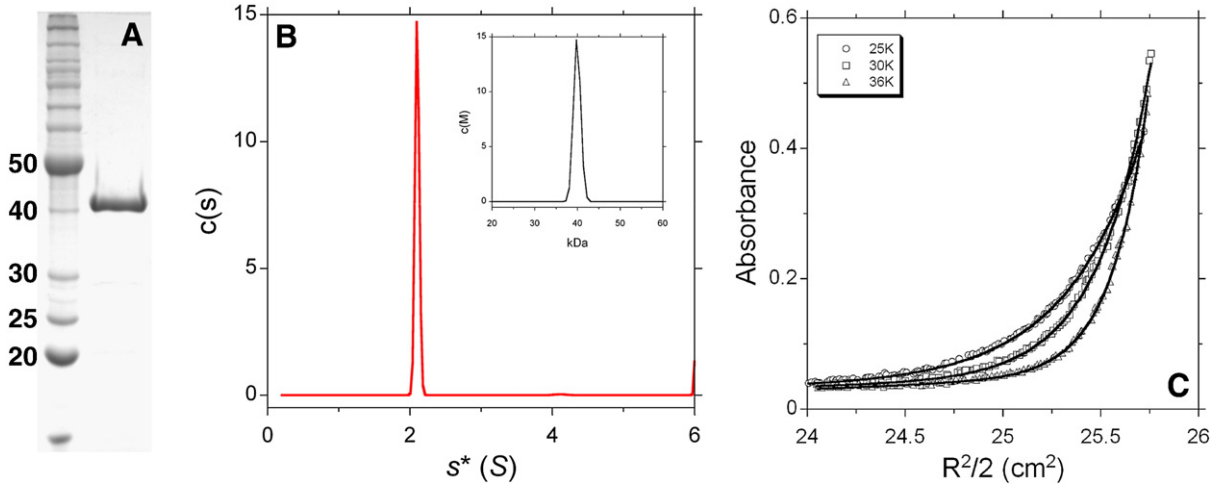


**Fig. 2.** *Quaternary structure of trIVa2 in solution.* A. SDS-PAGE gel showing the purified trIVa2. Lane1, molecular weight marker; Lane 2, 2.7 µg purified trIVa2. B. Sedimentation velocity experiment performed on purified trIVa2 (loading concentration of 3.4 µM, in Buffer H, at 25 °C. The data were analyzed using the SEDFIT program, and the resulting $c(s)$ distribution is shown. This analysis shows a single peak, indicating trIVa2 exists as a single species under these conditions. The data were converted to the corresponding $c(M)$ distribution, which showed a peak molecular weight at about 40 kDa, consistent with a monomer of trIVa2 (predicted molecular weight of 42.8 kDa). C. Sedimentation equilibrium experiment performed on the trIVa2 protein, under the identical solution conditions used in A. The rotor speeds used were 25, 30 and 36 k RPM. The resulting concentration gradients were analyzed according to an ideal, single species model, returning a molecular weight of 43±3 kDa, indicating trIVa2 exists as a monomer in solution.

methods. This DNA molecule is similar to the probes used in previous EMSA studies [27,29–31,34] that investigated the specific binding of IVa2 to DNA. To facilitate these studies, the 5′ end of the top strand was labeled with a Cy3 dye, which has an absorbance maximum at 550 nm. This wavelength allows us to monitor sedimentation of the DNA species, both free DNA and bound DNA, without signal contributions from the free trIVa2 protein.

First, sedimentation velocity experiments were performed by titrating a constant concentration of 1.25 μM A-I-II-Cy3 DNA with the trIVa2 protein, in Buffer H at 25 °C, and the mixtures were sedimented at 50K RPM and monitored at 522 nm (we chose to use 522 nm due to the increased lamp intensity at 522 when compared to 550 nm). The raw absorbance traces were analyzed using the $c(s)$ approach, and the resulting distributions are shown in Fig. 3A. For comparison, the top panel shows the $c(s)$ distributions obtained for the A-I-II-Cy3 DNA alone (solid line) and the trIVa2 protein alone (dashed line). The peak $s^*$ values are 2.65 S for the A-I-II-Cy3 DNA, and 2.06 S for the trIVa2. For the purposes of Fig. 3A, these values have not been corrected to standard conditions, since the binding stoichiometry must be known a priori to calculate the partial specific volume of the complex, which is needed to calculate the correction factor.

Upon mixing the trIVa2 and A-I-II-Cy3 samples a new peak appears in the $c(s)$ distribution centered at about 3.7 S. Furthermore, a concomitant decrease is observed in the $c(s)$ peak that corresponds to the free A-I-II-Cy3 DNA. Upon addition of between 2 and 2.5 μM trIVa2, the free DNA peak disappears completely. These data are consistent with the formation of a complex between the trIVa2 protein and the A-I-II-Cy3 DNA. Above 2.5 μM trIVa2, the 3.7 S peak shifts to higher $s$-values, and becomes more asymmetric. Continued addition clearly results in further binding of trIVa2 to the A-I-II-Cy3 DNA.

Considering the data collected in the trIVa2 concentration range of 0 to 2.5 μM, we see a linear increase in the weight averaged $s$ ($s_{wt}$; the average sedimentation coefficient observed for all species in solution [52,53]) with increasing trIVa2 protein concentration (Fig. 3B). This suggests the binding reaction, that results in the 3.7 S species, is stoichiometric under these solution conditions and protein/DNA concentrations, i.e. the total [A-I-II-Cy3] is much greater than the $K_d$ for this binding reaction. Consistent with this, the peak values in the $c(s)$ distributions that correspond to the free DNA and the trIVa2–DNA complex, do not change with increasing trIVa2 concentration up to about 2.5 μM trIVa2. This suggests that at a trIVa2 concentration between 2 and 2.5 μM, a single stoichiometric species is formed.

To further test this hypothesis, we repeated the sedimentation velocity experiments at a lower concentration of A-I-II-Cy3 DNA of 0.625 μM. This was the lowest concentration we could use for these experiments due to the low total absorbance of the sample. Fig. 3B shows that the $s_{wt}$ data collected at 1.25 μM A-I-II-Cy3 are linear with [trIVa2]/[A-I-II-Cy3] up to the highest trIVa2 concentration examined (6.25 μM). However, the data collected at 0.625 μM A-I-II-Cy3 DNA show an apparent break point at a loading ratio of trIVa2 to A-I-II-Cy3 DNA of [trIVa2]/[A-I-II-Cy3]=2. The most likely explanation for these data is that the additional binding that occurs at [trIVa2]/[A-I-II-Cy3]>2 occurs with a much lower affinity than the binding that occurs for [trIVa2]/[A-I-II-Cy3]<2. The fact that the data collected at the two [A-I-II-Cy3] overlay each other for [trIVa2]/[A-I-II-Cy3]<2 is further evidence this binding event is stoichiometric, and places an upper limit on the equilibrium dissociation constant for this reaction of about <100 nM.

There are two simple interpretations for the stoichiometry of this apparent 3.7 S species. Since the 3.7 S species saturates at about

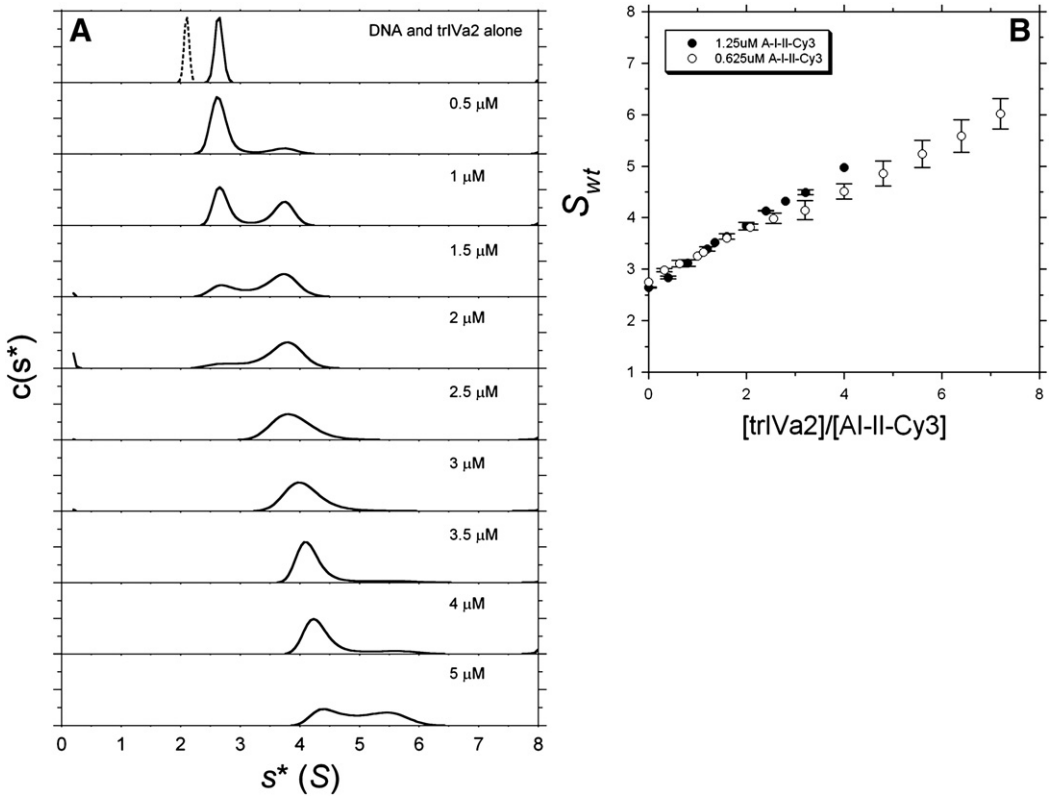


**Fig. 3.** *Determination of the binding stoichiometry of trIVa2 with the A-I-II-Cy3 DNA.* A. 1.25 μM of A-I-II-Cy3 was titrated with increasing concentrations of the trIVa2 protein, and the mixtures were studied by sedimentation velocity. The resulting $c(s)$ distributions are shown. The experiments were carried out at 522 nm, such that only the DNA molecule is detected. For comparison, the dashed line shows the $c(s)$ profile of the free trIVa2, obtained at 280 nm. The solid line in the top panel corresponds to the free A-I-II-Cy3 DNA. The free DNA peak disappears between 2 and 2.5 μM added trIVa2. B. The corresponding weight average sedimentation coefficients are plotted as a function of the loading ratio of trIVa2 to the A-I-II-Cy3 DNA. Experiments were performed at either 1.25 or 0.625 μM total A-I-II-Cy3 concentration. Error bars correspond to standard deviations calculated from at least three separate experiments.

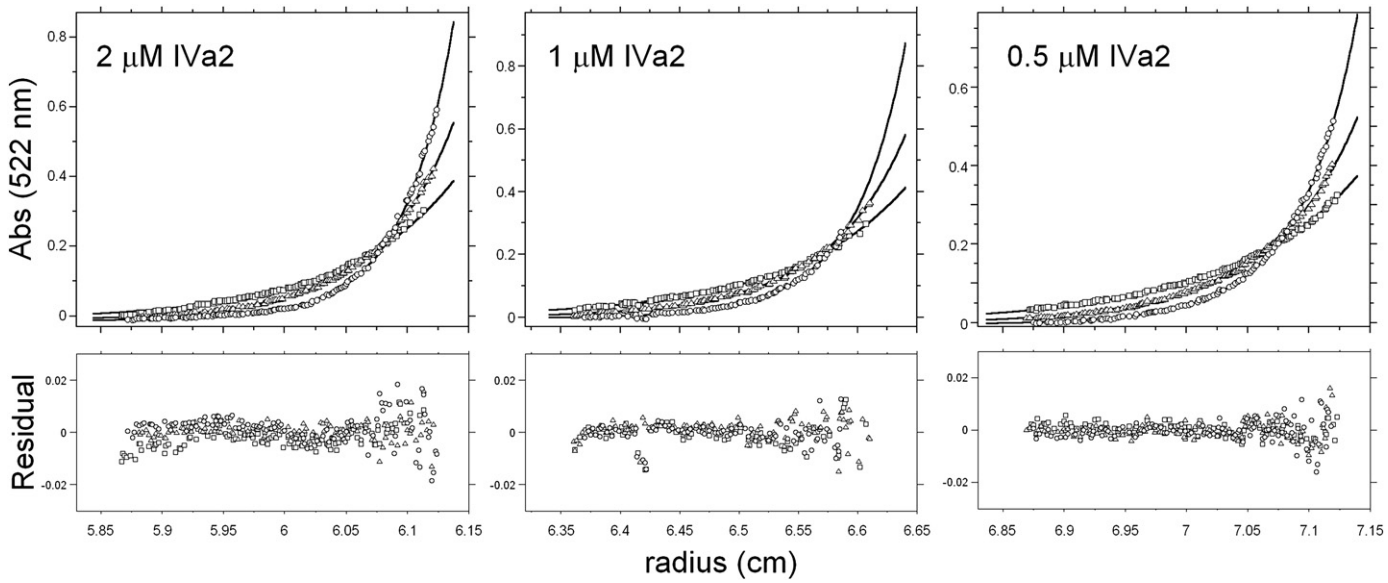


**Fig. 4.** *Determination of the size of the 3.7 S species by sedimentation equilibrium*. Three loading ratios of trIVa2 to A-I-II-Cy3 DNA were examined each at three rotor speeds (14, 17 and 21K RPM), in Buffer H at 25 °C. The total A-I-II-Cy3 concentration was held constant at 1.25 μM, while the trIVa2 concentration was varied as indicated in the figure. The data were globally analyzed by NLLS according to Eq. (1) from the text. The simulations were calculated starting from the sample meniscus ($r_m$) and finishing at the base of the cell ($r_b$). The bottom panels show the residuals of the fit for each trIVa2 loading concentration.

2.5 μM trIVa2, this might indicate this species corresponds to two trIVa2 proteins bound to one A-I-II-Cy3 DNA, i.e. a 2:1 binding stoichiometry. Alternatively, if the DNA binding activity of the trIVa2 protein preparation is around 50%, then the 3.7 S species might correspond to a 1:1 binding stoichiometry.

To determine which of these possibilities is correct, we performed sedimentation equilibrium experiments at [trIVa2]/[A-I-II-Cy3]≤2, to measure the molecular weight of the protein–DNA complex that is formed. The results of these experiments are shown in Fig. 4. Since the binding reaction is stoichiometric under these conditions, and since we see two, well defined peaks in the $c(s)$ distributions, as discussed above, we expect to see two species in the sedimentation equilibrium experiments. One species should correspond to the free A-I-II-Cy3 DNA, while the other should correspond to the 3.7 S species.

Sedimentation equilibrium experiments (not shown) performed on the A-I-II-Cy3 DNA alone showed the DNA sedimented as a single, ideal species yielding a buoyant molecular weight of 12.89±0.26 kDa. Based on the DNA sequence, the predicted molecular weight of the DNA (including the Cy3 dye) is 30,039 Da. From these values, we calculate (see Section 2.4) a partial specific volume for the DNA molecule of 0.5525±0.0083 mL/g. The partial specific volume of duplex DNA is commonly taken as 0.55 mL/g [43], and a number of studies have measured similar values using AUC techniques (for example, see Bonifacio et al. [48], who report an average value of 0.56±0.015 mL/g in 0.1 M KCl).

Next, increasing concentrations of the trIVa2 protein of 0.5, 1 and 2 μM, were added to 1.25 μM A-I-II-Cy3 DNA, and the mixtures were sedimented until they reached equilibrium at three rotor speeds of 14, 17 and 21K RPM. If the 3.7 S species observed in the $c(s)$ distributions corresponds to a 1:1 binding stoichiometry, we would expect to observe a trIVa2–DNA species with a buoyant molecular weight of 22.9 kDa (see Section 2.4 for buoyant molecular weight calculations). On the other hand, if the 3.7 S species corresponds to a 2:1 binding stoichiometry, we would expect to observe a species with a buoyant molecular weight of 33.0 kDa.

The data shown in Fig. 4 were analyzed by NLLS using a model that assumes two, ideal species are present in solution, and that the binding reaction is stoichiometric between the trIVa2 and the A-I-II-Cy3 DNA molecules (see Eq. (1) in Section 2.4). At 522 nm, the only absorbing species present in these experiments is the A-I-II-Cy3 DNA, therefore the absorbance profiles shown in Fig. 4 reflect either free DNA or DNA that is bound to the trIVa2.

The smooth curves shown are the results of simulations using the best fit parameters from the NLLS analysis. In this analysis, the buoyant molecular weight for the free DNA was fixed at its previously determined value of 12.89 kDa, while the buoyant molecular weight of the bound species was allowed to float, which returned a best fit value of 22.8±1 kDa. Therefore, this experiment conclusively indicates the protein preparation is approximately 50% active for DNA binding, under these experimental conditions.

### 3.3. Quantification of the A-I-II DNA binding activity of the trIVa2 preparation

Since we determined that the 3.7 S species corresponds to a single trIVa2 bound to the A-I-II-Cy3 DNA, we were able to further analyze the sedimentation velocity data directly by NLLS methods using a model that contained only two sedimenting species; as discussed above, one of which corresponds to the free DNA and the other to the 1:1 trIVa2–DNA complex. Since we had determined the size of the trIVa2–DNA complex, by fixing the equilibrium association constant for the trIVa2–DNA binding reaction to a value large enough to ensure stoichiometric binding conditions, we could float the total trIVa2 concentrations to get a direct measure of the protein binding activity. Even though the trIVa2 does not contribute to the total absorbance at 522 nm, these total protein concentration amplitude terms were well determined in the NLLS analysis because the increase in the rate of sedimentation upon titration of A-I-II-Cy3 DNA with trIVa2 is attributed to the formation of a 1:1 trIVa2–DNA complex. Furthermore, only the fraction of trIVa2 that is competent to bind the DNA is detected; thus the fitted values one obtains from this analysis correspond to the active total trIVa2 concentration.

Fig. 5 shows the results of a global fit, using the SEDPHAT program, of sedimentation velocity data collected for 6 concentrations of added trIVa2, for total [trIVa2]/[A-I-II-Cy3]≤2. The results of this analysis clearly show this model describes the data very well. The fitted $s_{20,w}$ values for the free DNA and the 1:1 trIVa2–DNA complex are 3.50± 0.09 and 4.92±0.09 S, respectively, which correspond to 2.68±0.07 and 3.66±0.07 S uncorrected to standard conditions. These values are

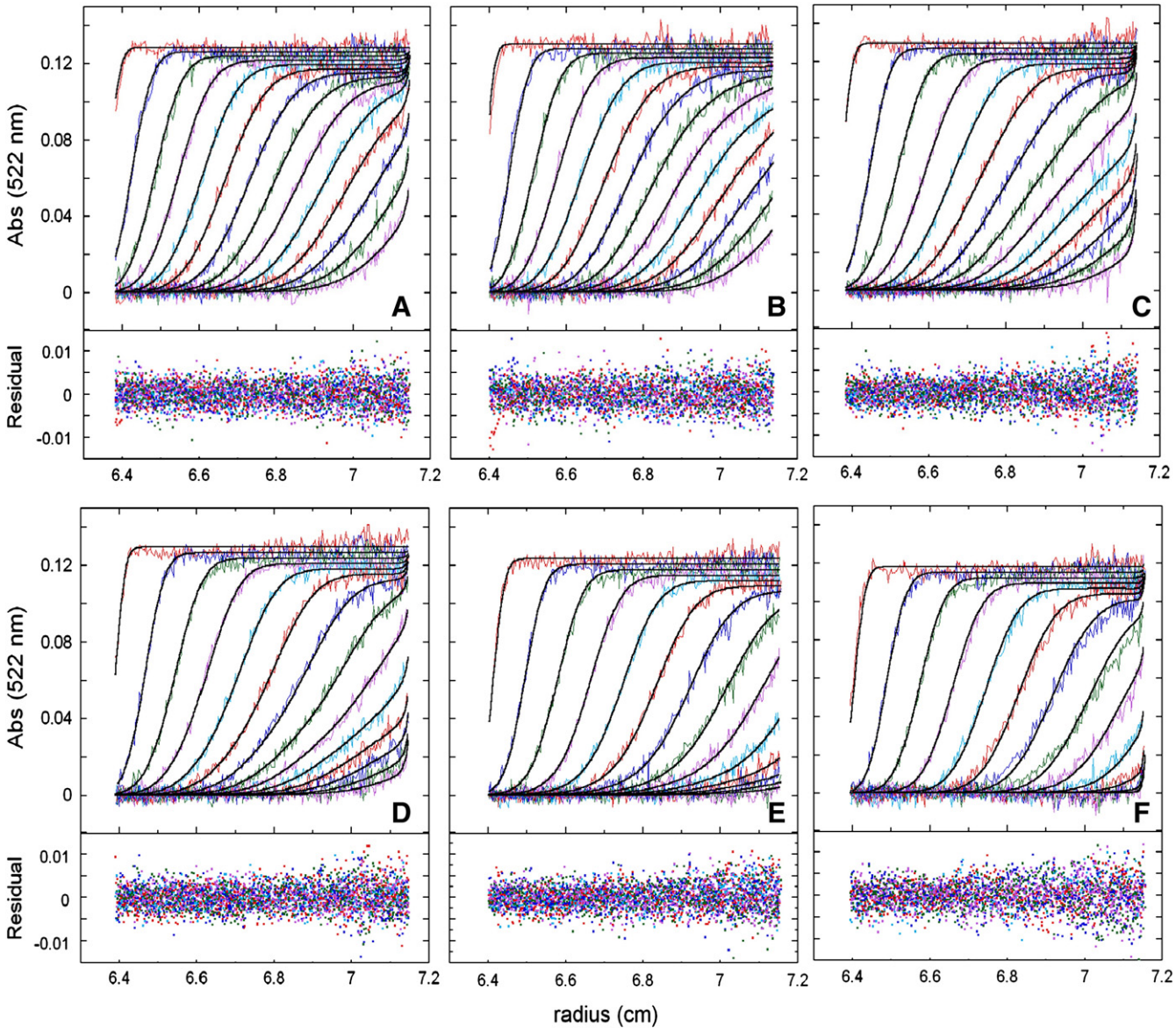


**Fig. 5.** *Global analysis of sedimentation velocity data for the formation of the 1:1 trIVa2/A-I-II-Cy3 complex.* A constant concentration of the A-I-II-Cy3 DNA of 1.25 μM was incubated with increasing concentrations of the trIVa2 protein, corresponding to 0, 0.5, 1, 1.5, 2, 2.5 μM trIVa2 protein, for panels *a* through *f*. For ease of presentation, an experiment performed at 1.69 μM trIVa2, while included in the global analysis, is not shown, and only every third scan is shown. The bottom panels are the residuals resulting from the global NLLS analysis. The data were fitted to a two-species, stoichiometric binding model using SEDPHAT. The analysis returned $s_{20,w}$ values for the free DNA and the 1:1 DNA-trIVa2 complex of 3.50 ± 0.09 and 4.92 ± 0.09 S.

very similar to those estimated from the peaks of the $c(s)$ distributions (2.65 and 3.7 S) obtained for data collected at [trIVa2]/[A-I-II-Cy3] ≤ 2. Fig. 6 shows a plot of the fitted values of the total trIVa2 concentration competent to bind the A-I-II-Cy3 DNA, as a function of the total, known loading concentration of trIVa2.

Since the sedimentation equilibrium data presented in Fig. 4 were analyzed using the mass conservation approach, we were able to estimate the total trIVa2 concentration competent to bind the A-I-II-Cy3 DNA, in each channel of data (see Supplementary data, section *S.1*). These data are also included as open triangles in Fig. 6. This comparison shows the same protein activity is measured regardless of which technique, sedimentation velocity or equilibrium, is used. Since a typical sedimentation equilibrium experiment takes several days to complete, while a typical sedimentation velocity experiment takes several hours, this also indicates the trIVa2 protein retains its DNA binding activity for up to ~4.5 days at 25 °C, in Buffer H. When all the data are combined and analyzed by LLS, the final protein activity is estimated as 53 ± 2%. We have estimated a similar value for four different trIVa2 protein preparations.

Experiments discussed in Section 3.5 show that the trIVa2 protein also binds with relatively high affinity to non-specific DNA. At 1.25 μM of a non-specific 48mer DNA, this binding reaction occurs under stoichiometric conditions, however, the overall affinity for non-specific binding is weaker than it is for specific binding. This observation suggested we could use double stranded DNA cellulose methods to further test our conclusion that about half of our protein preparation is inactive for DNA binding.

At first, we poured a small, 250 μL gravity flow column, using the dsDNA cellulose material (at 0.63 mg DNA/mL column material, see Section 2.7) and equilibrated the column in Buffer H at 25 °C. Then we loaded 0.225 mg of trIVa2 onto the column, in Buffer H at 25 °C. The mass ratio of protein to DNA was 1.42, which is identical to a binding experiment carried out at 1.25 μM total trIVa2 protein and 1.25 μM A-I-II-Cy3 DNA (42,767 g/mol of trIVa2 divided by 30,039 g/mol of A-I-II-Cy3). At these very high DNA concentrations (about 16.8 fold higher than the DNA concentrations used in the AUC experiments), all of the trIVa2 protein bound to the DNA column,

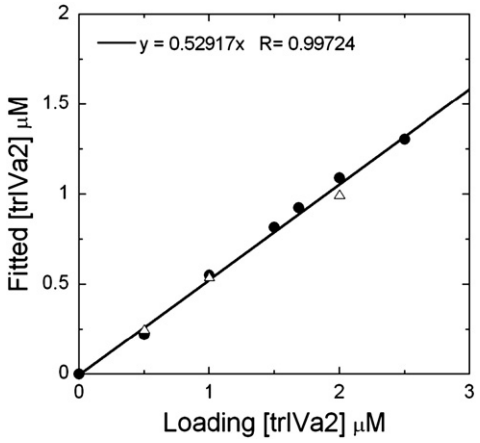


**Fig. 6.** *Determination of the DNA binding activity of the trIVa2 protein preparation*. The closed circles correspond to the best fit total trIVa2 concentration parameters from the global, NLLS analysis of the raw sedimentation velocity data shown in Fig. 5. The open triangles correspond to the best fit total trIVa2 concentration obtained from the global, NLLS analysis of the sedimentation equilibrium data shown in Fig. 4. In both cases, the best fit concentration is plotted against the known, total loading concentration of the trIVa2 protein, which was calculated based on UV absorption spectroscopy, as discussed in Section 2.1. The solid line is the result of linear least squares fit of all the data, and yields an activity for the trIVa2 protein preparation of 53%.

and we were able to elute all the protein by washing the column with Buffer H+0.5 M NaCl (data not shown). At these high DNA concentrations, it is likely the "inactive" trIVa2 conformation associates with the ds DNA through electrostatic interactions; the calculated p*I* of the trIVa2 protein is 8.86, therefore, the inactive trIVa2 conformation is predicted to be positively charged in Buffer H (pH 7.6). This is the same reason the inactive conformation binds tightly to the SP Sepharose column (which is a negatively charged column) during the protein purification procedure.

Based on this result, we designed an experiment to investigate the binding of trIVa2 to the dsDNA cellulose material under the 16.8 fold lower DNA concentrations used in the AUC experiments. For this experiment, we added 37.5 μg/mL double stranded DNA cellulose material (where 37.5 μg/mL refers to the total DNA concentration) to 1.25 μM trIVa2 protein (53.5 μg/mL), in Buffer H. The concentration 37.5 μg/mL corresponds to the same concentration (1.25 μM) of the A-I-II-Cy3 DNA ($1.25\times10^{-6}$ M*30,039 g/mol=37.5 μg/mL) used in the AUC experiments. The mixture was allowed to incubate at 25 °C for 15 min with frequent hand-mixing. The dsDNA cellulose material was pelleted using a low-speed desktop centrifuge, and an aliquot of the supernatant was taken for subsequent SDS-PAGE analysis (lane 1, Fig. 7). The dsDNA cellulose material was resuspended and pelleted three more times with Buffer H (lanes 2–4, Fig. 7). Next, the dsDNA cellulose was resuspended and pelleted three times with Buffer H+0.5 M NaCl (lanes 5–7). Based on the AUC experiments, we expect that about 50% of the trIVa2 protein will bind to the dsDNA cellulose material (the active conformation), in Buffer H, while about 50% will be found in the Buffer H wash fractions (the inactive conformation). Indeed, we see that not all of the trIVa2 protein is competent to bind the ds DNA cellulose material (see fractions 1–4 of Fig. 7), while a fraction of the protein is retained on the ds DNA cellulose material, and is eluted with the 0.5 M NaCl wash. The band intensity shown in lane 1 should be multiplied by a factor of four, since the total volume of sample present in the initial incubation (400 μL) was 4 times that observed in each subsequent wash (100 μL). These results are consistent with our conclusion that the trIVa2 purified for this work exists in two forms, one of which has high affinity DNA binding activity, while the other has no (or at least very weak) DNA binding activity. Whether this observation is simply an artifact of the purification procedure utilized in this work, or if this represents two biologically relevant forms of the trIVa2 protein, awaits further experimentation.

### *3.4. Modeling the binding of a second trIVa2 monomer onto the trIVa2/A-I-II-Cy3 complex*

As mentioned earlier, it is clear that additional trIVa2 binds the A-I-II-Cy3 DNA, beyond the 1:1 stoichiometry demonstrated, although with much weaker affinity than the first binding event, which produces the 1:1 complex. To further explore this binding event, we performed sedimentation equilibrium experiments at [trIVa2]/[A-I-II-Cy3] of 2.8 and 3.6, which correspond to total trIVa2 concentrations of 3.5 and 4.5 μM, respectively. Using our estimate of the DNA binding protein activity of 53%, this corresponds to [trIVa2]/[A-I-II-Cy3] of 1.48 and 1.91. We have had difficulty exploring higher concentrations, due to solubility issues in the current buffer.

These data are not sufficient to determine the precise size of the trIVa2 complex formed beyond the 1:1 complex. Therefore, we have assumed this second binding event corresponds to the formation of a 2:1 trIVa2 to DNA complex, and have estimated the equilibrium association constant for this reaction. This was possible since this binding event was not stoichiometric (its affinity was not too strong). Furthermore, since we analyzed the data using the mass conservation approach, knowledge of the total active protein concentration can be used in the analysis to estimate the equilibrium association constant, even though the free protein concentration is not directly detected in the experiments (see Supplementary data, section *S.1*). This analysis resulted in an equilibrium dissociation constant for this additional binding event of 1.4±0.7 μM (Fig. 8). This value is ~14 fold weaker than the upper limit (<100 nM) estimated for the equilibrium dissociation constant for formation of the 1:1 complex.

### *3.5. Specificity of binding of the recombinant trIVa2 protein with the A-I-II DNA*

To determine if the trIVa2 protein binds to the A-I-II-Cy3 DNA with specificity, we performed competition experiments using the sedimentation velocity approach. For these experiments, we incubated 2 μM trIVa2 (which corresponds to 1.06 μM active trIVa2) with 1.25 μM A-I-II-Cy3 DNA, along with increasing concentrations of a competitor DNA. Two competitor DNAs were investigated. The first was an unlabeled A-I-II DNA, which was otherwise identical to the A-I-II-Cy3 DNA. The second was an unlabeled mutant DNA, called A-I-II-mut, where both TTTG sequences were changed to ACAC and both CGXG sequences were changed to ATXC, while the remaining sequence was identical to the A-I-II-Cy3 DNA (see Fig. 1).

Fig. 9 shows the dependence of the weight averaged sedimentation coefficient ($s_{wt}$) on increasing concentration of competitor DNA, at a constant concentration of trIVa2 and A-I-II-Cy3 DNA. These data show that the A-I-II DNA competes for trIVa2 binding to the A-I-II-Cy3 DNA more effectively than the A-I-II-mut. These data were analyzed by

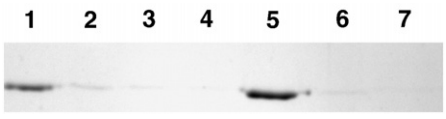


**Fig. 7.** *Separation of active and inactive trIVa2 by dsDNA chromatography.* SDS-PAGE gel showing the results of the batch separation of the inactive and active fractions of the trIVa2 protein. Lane 1, supernatant from the Buffer H+trIVa2 incubation. Lanes 2–4, three consecutive Buffer H washes. Lanes 5–7, three consecutive Buffer H+0.5 M NaCl washes. For comparison, the intensity of the band in lane 1 should be multiplied by a factor of four.

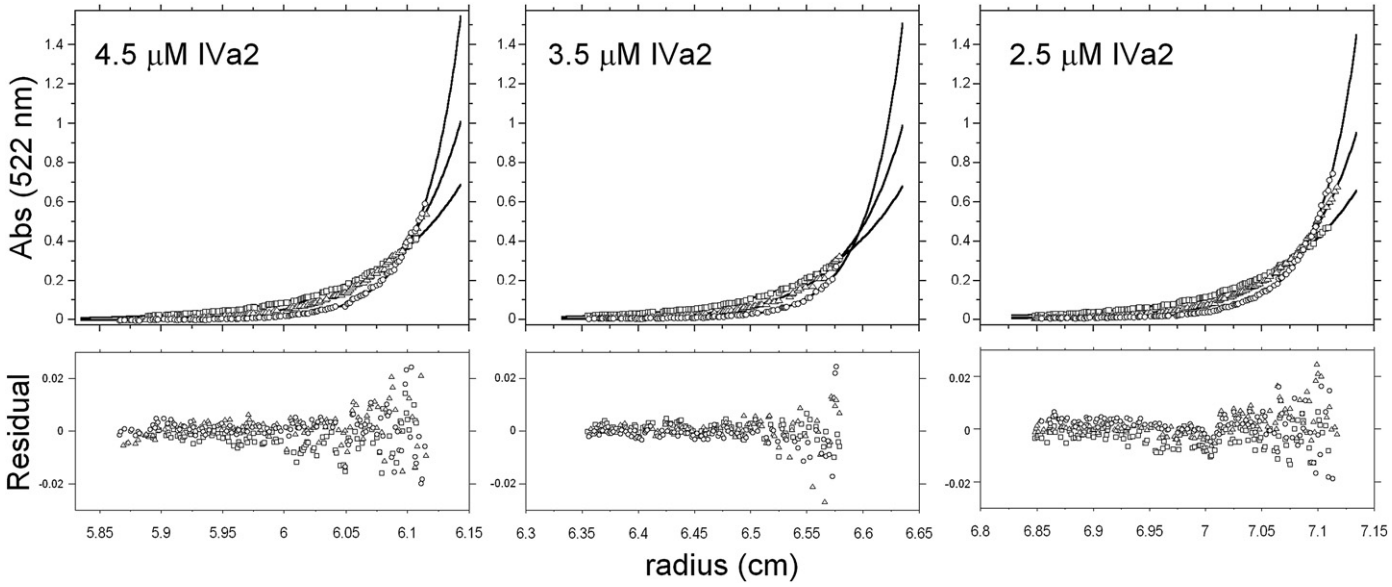


**Fig. 8.** *Determination of the equilibrium dissociation constant for the binding of a second trIVa2 monomer to the 1:1 trIVa2/A-I-II-Cy3 complex.* Three loading ratios of trIVa2 to A-I-II-Cy3 DNA were examined each at three rotor speeds (14, 17 and 21K RPM), in Buffer H at 25 °C. The total A-I-II-Cy3 DNA loading concentration was held constant at 1.25 μM. The data were globally analyzed by NLLS methods, using the Scientist software, according to Equations S12–S14, as discussed in the Supplementary data. The simulations were calculated starting from the sample meniscus ($r_m$) and finishing at the base of the cell ($r_b$). The bottom panels show the residuals of the fit for each trIVa2 loading concentration. The best-fit value for $K_2$ was 0.71 ± 0.36 $\mu M^{-1}$, which corresponds to a $K_d$ of 1.4 ± 0.7 μM.

NLLS using Eq. (2) (see Section 2.5 and Supplementary data, section *S.2*), which was derived for a 1:1 binding stoichiometry where an unlabeled, competitor DNA competes for binding of the trIVa2 protein to the labeled, A-I-II-Cy3 DNA, and both binding events are stoichiometric, i.e. the free protein concentration is always much less than the total bound protein concentration. Thus, competition experiments performed using either unlabeled A-I-II DNA or the A-I-II-mut DNA as competitors for binding to the reference, A-I-II-Cy3 DNA allowed us to quantify the equilibrium association constant ratios $K_{A\text{-}I\text{-}II}/K_{A\text{-}I\text{-}II\text{-}Cy3}$, $K_{A\text{-}I\text{-}II\text{-}mut}/K_{A\text{-}I\text{-}II\text{-}Cy3}$, and $K_{A\text{-}I\text{-}II}/K_{A\text{-}I\text{-}II\text{-}mut}$. It is important to point out that even though these ratios can be determined, the individual equilibrium constants cannot be determined unless the experiments are carried out under much lower total DNA, competitor and protein concentrations [54]. Analysis of these data yields $K_{A\text{-}I\text{-}II}/K_{A\text{-}I\text{-}II\text{-}Cy3} = 0.56 \pm 0.07$, $K_{A\text{-}I\text{-}II\text{-}mut}/K_{A\text{-}I\text{-}II\text{-}Cy3} = 0.055 \pm 0.010$. From these two ratios, we can then account for the presence of the Cy3 dye, to determine if the increased affinity for the A-I-II-Cy3 DNA is due to the presence of the dye molecule. Dividing these two ratios yields $K_{A\text{-}I\text{-}II}/K_{A\text{-}I\text{-}II\text{-}mut} = 10 \pm 1$. From this analysis it is clear the recombinant, truncated IVa2 protein studied here binds with some specificity to the A-I-II DNA.

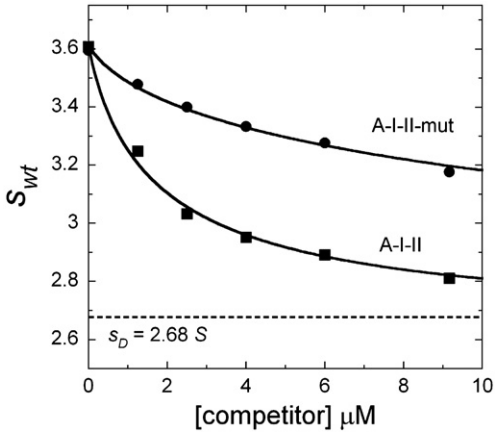


**Fig. 9.** *Determination of the specificity of binding of the trIVa2 protein to the A-I-II-Cy3 DNA.* 2 μM total trIVa2 (1.06 μM active trIVa2) was mixed with 1.25 μM A-I-II-Cy3 DNA along with increasing concentrations of the indicated competitor DNA. The data were analyzed according to Eq. (2), and the results are shown as smooth curves drawn through the data. The values of $s_D$ and $s_{PD}$ are fixed in the analysis, and are taken from the results of the global, NLLS analysis of the raw sedimentation velocity data studying the binding of trIVa2 to the A-I-II-Cy3 DNA shown in Fig. 5. The dashed line corresponds to the expected *s*-value for the free DNA (un-corrected to standard conditions), which is 2.68 S.

Even though trIVa2 binds with higher affinity to the specific A-I-II DNA, it also appears to bind with a relatively high affinity to DNA without the A repeats. Therefore, we performed sedimentation equilibrium experiments to investigate the binding of trIVa2 to the A-I-II-mut-Cy3 DNA, under the identical conditions used to study trIVa2 binding to the A-I-II-Cy3 DNA (data not shown).

These experiments show that at 1.25 μM loading concentration of the A-I-II-mut-Cy3 DNA, the binding reaction is stoichiometric. The buoyant molecular weight of the trIVa2–DNA complex is 24 ± 1 kDa, which is the same, within error, to that determined for the binding of the trIVa2 with the A-I-II-Cy3 wildtype DNA. Since we know that formation of the 1:1 complex, on the A-I-II-mut-Cy3 DNA, is stoichiometric at 1.25 μM DNA concentration, and since we have measured the ratio of equilibrium constants for this binding reaction, we can further extend the upper limit for the $K_d$ for formation of the 1:1 trIVa2/A-I-II DNA complex to ~10 nM. Thus, the equilibrium dissociation constant for formation of the 1:1 trIVa2/A-I-II DNA complex is less than about 10 nM. EMSA experiments looking at binding of purified, full length IVa2 to a similar A-I-II DNA, estimated a $K_d$ of about 11 nM [30], although these experiments were performed under very different solution conditions (20 mM HEPES, pH 8, 10 mM Mg acetate, 5 mM KCl, 0.5 mM EDTA, 1 mM DTT and 12% glycerol, at 23 °C).

The binding of trIVa2 to the non-specific, A-I-II-mut-Cy3 DNA was also investigated using the sedimentation velocity technique, in Buffer H at 25 °C. Increasing concentrations of trIVa2 were added to a constant concentration of A-I-II-mut-Cy3 DNA, and parallel experiments were performed using the A-I-II-Cy3 DNA. The resulting $c(s)$ distributions are shown in Fig. 10. In all cases, the $c(s)$ distributions are significantly more broad for the A-I-II-mut-Cy3 DNA than they are for the wildtype DNA. This result suggests the trIVa2 forms a wider range of structures on the mutant DNA than it does on the wildtype DNA,

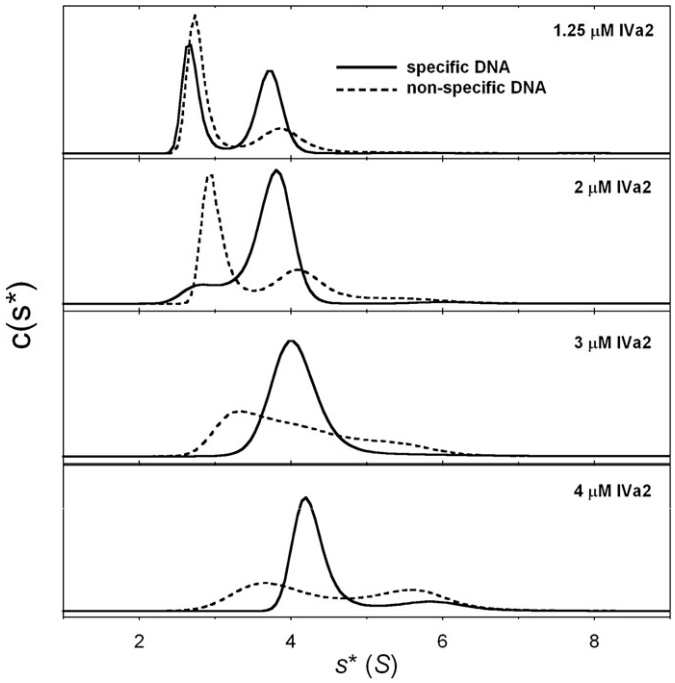


**Fig. 10.** *Comparison of specific vs. non-specific binding of trIVa2 to DNA*. The *c*(*s*) distributions obtained for trIVa2 binding to either the A-I-II-Cy3 DNA (specific, solid line) or the A-I-II-mut-Cy3 DNA (non-specific, dashed line) are shown. For both cases, the protein and DNA concentrations are much greater than the $K_d$ for the 1:1 binding reaction, thus the reaction occurs under stoichiometric conditions. In all cases, the *c*(*s*) distribution for the A-I-II-Cy3 DNA is less broad than for the A-I-II-mut-Cy3 DNA, indicating the trIVa2 interacts with the A-I-II-Cy3 DNA in a fundamentally different ways than it does with the mutant DNA. It is most likely the case that the trIVa2 can bind to multiple locations on the mutant DNA, as a non-specific DNA binding protein would, while it interacts with the A-I-II DNA in a specific way, resulting in a smaller number of conformations on this DNA.

which results in a broader distribution of *s* values required to describe the sedimentation velocity raw data. This also prevents us from analyzing the sedimentation velocity data obtained for the A-I-II-mut-Cy3 DNA directly; we can't simply assign a single sedimentation coefficient to the trIVa2–DNA complex, since there are likely many ways the 1:1 complex form, each of which having a different *s*-value. This result provides additional evidence the trIVa2 interacts with the DNA with the A repeats in a fundamentally different way than it does with DNA that contain no A repeats. Furthermore, since we do observe additional trIVa2 binding to the A-I-II-Cy3 DNA, albeit at a much lower affinity than the first, stoichiometric binding event, and since the first binding event with the mutant DNA occurs with high affinity, it seems likely there is significant negative cooperativity associated with putting two trIVa2 proteins onto one A-I-II-Cy3 DNA.

## 4. Discussion

The viral DNA packaging reaction in Ad requires specific binding of the IVa2 and L4-22K proteins to the PS DNA [23,27,28,31,34,36,37,55]. Furthermore, the binding of the L4-22K protein to the PS DNA requires IVa2, while IVa2 binding to the PS DNA does not require L4-22K [29,34]. Presumably, this interaction signals either the linear translocation of the viral DNA into the interior of a preformed viral capsid or signals the assembly of the viral capsid around the condensed, viral DNA. Despite intensive study, the molecular details of the interaction of IVa2 with the PS DNA have not been determined. In this work, we have begun a physical–chemical study of the binding of the IVa2 protein to a DNA molecule containing A repeats I and II, to begin to understand how IVa2 interacts with the full PS DNA, and to eventually understand how the IVa2 and L4-22K protein interact together with the PS DNA to signal viral DNA packaging.

### 4.1. Stoichiometry of the trIVa2/A-I-II binding reaction

Initial experiments showed that the purified trIVa2 protein exists as a monomer in solution, under the conditions used in this work. This result is consistent with a previous study that investigated the self-association of full-length IVa2 using the glycerol gradient sedimentation velocity technique [25].

Next, we used sedimentation velocity and equilibrium methods to investigate the stoichiometry of the interaction of the recombinant, trIVa2 monomer with a DNA that contained A repeats I and II (A-I-II). Although previous EMSA experiments identified a single gel-shifted band when studying the binding of the IVa2 protein with a DNA probe that contained the A-I and II repeats, this does not necessarily imply that a single IVa2 protein interacts with the DNA molecule. One possibility is that multiple IVa2 proteins can interact with the DNA in a highly cooperative fashion, so that only a single, higher order protein–DNA complex is formed; a hallmark of cooperative assembly is the suppression of lower order intermediate states. A second possibility is that weak protein–DNA interactions are not detected due to the non-equilibrium nature of the EMSA technique.

The experiments presented in this work showed that a single trIVa2 monomer bound with high affinity ($K_d < \sim 10$ nM) to the A-I-II DNA. We also observed the formation of a complex larger than 1:1, at high enough trIVa2 concentrations, although we have not been able to determine its precise size due to solubility issues of the trIVa2 protein in the current buffer. If we assume that this larger complex corresponds to the formation of a 2:1 trIVa2 to DNA ligation state, we can estimate the $K_d$ for the binding of the second trIVa2 to the 1:1 trIVa2–DNA complex to be 1.4 ± 0.7 μM. Since we determined the trIVa2 protein binds to the specific A-I-II DNA with a 10 fold higher affinity than it does to a DNA lacking the consensus TTTG and CG motifs, we can extend the upper limit for the $K_d$ for formation of the 1:1 trIVa2-non-specific DNA complex to ~100 nM. Thus, binding of a trIVa2 monomer to a DNA that is expected to be non-specific is more favorable than binding a second trIVa2 monomer to the specific A-I-II DNA. This result suggests the second trIVa2 binds to the A-I-II DNA with significant negative cooperativity. If we assume that the first trIVa2 binding event, which forms the 1:1 complex, can occur at either the A-I or A-II repeat, and that the site-specific affinity at either site is identical, we can put an *upper limit* on the cooperativity constant of ~0.002, which corresponds to a cooperative free energy of ~+3.7 kcals/mol. Thus, there is an energetic penalty associated with placing two trIVa2 molecules on adjacent A repeats. An attractive hypothesis is that the L4-22K protein may play a role in modulating this energetic penalty; we are currently exploring the role the L4-22K protein may play in this interaction.

Previous experiments have been reported that examined the binding stoichiometry of the IVa2 protein with the DE element [25], although no previous experiments have been reported that have examined the binding stoichiometry of the IVa2 protein with DNA containing A repeats. IVa2 binds specifically to the DE element present within the Major Late Promoter, and stimulates transcription from this promoter. The authors used protein–DNA crosslinking experiments, as well as glycerol gradient sedimentation experiments, to study the size of the complex that forms between the IVa2 protein and a DNA probe that contains the DE element. The authors interpreted these experiments to show that a dimer of IVa2 bound to the DE element, although it should be noted these techniques do not necessarily report on the equilibrium distribution of the protein–DNA species that are formed in solution. In spite of this potential difficulty, it is possible the dimer we have observed in our experiments corresponds to the same dimer observed in these earlier experiments [25].

### 4.2. Sequence-specific binding of the trIVa2 protein to the A-I-II DNA

Previous EMSA experiments have demonstrated that IVa2 has a higher affinity for DNA that contains A repeats than for non-specific

DNA [30,31]. In this work we have measured the specificity ratio for the trIVa2 protein, which quantifies the ratio of equilibrium association constants for specific and non-specific DNA binding. While it is clear the trIVa2 protein interacts with the A-I-II (specific) DNA in a fundamentally different way than it does with non-specific DNA, the recombinant trIVa2 protein used here does not show a large degree of sequence specificity for the A-I-II DNA, when compared to non-specific DNA of the same length, since it binds with only a 10-fold lower $K_d$ to the A-I-II DNA than it does to a non-specific DNA. For comparison, the specificity ratio for λ cI repressor binding to its operator site [56] is ~$10^7$. Another, less extreme example is the *E. coli* Integration Host Factor [57], which has a specificity ratio of ~150, although it should be emphasized these values depend upon solution conditions. The relatively low specificity ratio measured here may be due to the fact that we are studying a truncated version of the IVa2 protein, although we point out this protein still supports production of infectious Ad particles [28]. It is also possible post-translational modifications of IVa2 modulate its DNA binding affinity. Further studies are needed to understand how IVa2 specifically interacts with the DE and PS elements.

### *4.3. Hydrodynamic properties of the trIVa2 protein, the A-I-II-Cy3 DNA, and the trIVa2/A-I-II-Cy3 complex*

The frictional coefficient ratio, $f/f_0$, for the trIVa2 protein was calculated from the measured sedimentation coefficient to be 1.29±0.01 (see Section 2.6). This ratio is calculated by dividing the experimentally determined frictional coefficient of the macromolecule, $f$, by the predicted frictional coefficient of a hydrated sphere of identical mass and partial specific volume, $f_0$. If the macromolecule possesses an approximately spherical shape, $f/f_0$ will have a value close to 1. The measured value for the trIVa2 protein indicates the protein has an elongated structure in solution. If the overall shape of trIVa2 is modeled as a prolate ellipsoid, the corresponding axial ratio (the major axis divided by the minor axis [43]) is calculated to be 5.6±0.2. Using the calculated hydration of trIVa2 of 0.3789 g/g (see Section 2.6), the hydrated volume of the protein can be calculated according to [49] $V_{hyd} = (\delta/\rho + \upsilon)(M/N_{av})$. Since the volume of a prolate ellipsoid is given by $V_{pro} = 4/3\pi ab^2$, and since the axial ratio, $a/b$, is known, the overall hydrated dimensions of the trIVa2 protein, assuming a prolate ellipsoid shape, can be calculated. This calculation yields $a = 8.4 \pm 0.2$ nm, and $b = 1.50 \pm 0.02$ nm. Comparison of these dimensions to those calculated for the 48 bp A-I-II-Cy3 DNA, we see that it is possible the trIVa2 protein may be as long as the A-I-II-Cy3 DNA (compare 16.8±0.4 nm for the trIVa2 protein with 0.337 nm/bp*48 bp=16.2 nm calculated for the DNA). Therefore, it is possible a single monomer of trIVa2 can simultaneously interact with both A repeats present in the A-I-II-Cy3 DNA. Based on these calculations, it seems possible simple steric considerations may explain the apparent large, energetic penalty for placing two trIVa2 monomers on a single A-I-II DNA molecule.

Using the $s_{20,w}$ of 4.92±0.09 S calculated for the 1:1 trIVa2/A-I-II-Cy3 complex, we calculate an $f/f_0$ of 1.35±0.03. To calculate this value, we assumed we could accurately estimate the overall hydration of the complex according to a simple weight averaged calculation (see Section 2.6). Using a prolate ellipsoid model, we calculate an axial ratio for the 1:1 complex of 6.6±0.5, indicating the structure of the complex adopts an extended conformation. Using the same method as described above, the overall dimensions of the complex are estimated as $a = 11.4 \pm 0.6$ nm and $b = 1.73 \pm 0.05$ nm. This calculation suggests the length of the complex (22.8±1.2 nm) is greater than that of the A-I-II-Cy3 DNA by itself. This may indicate the trIVa2 protein interacts with the A-I-II-Cy3 DNA such that a segment of the protein extends over the edge of the DNA, adding to the overall length of the complex. Comparison of the axial ratios of the free trIVa2 (5.6±0.2), the free A-I-II-Cy3 DNA (16.2/2.25=7.2±0.5) and the 1:1 complex (6.6±0.5), suggests the resulting complex does not involve a large degree of DNA wrapping around the trIVa2 protein, since this likely would result in a more compact, spherical structure, which is inconsistent with the calculated axial ratio of the complex. Furthermore, the axial ratio of the complex falls between the calculated values of the free trIVa2 and A-I-II-Cy3 molecules. This is consistent with an essentially rigid-body association between the two structures.

## Acknowledgements

N. K. Maluf thanks Dr. Mike Feiss for encouragement and advice during the beginning of this project. We thank Dr. David Bain for insightful discussions during the course of this work. This work was supported by start-up funds provided by the Department of Pharmaceutical Sciences, University of Colorado Denver.

## Appendix A. Supplementary data

Supplementary data associated with this article can be found, in the online version, at doi:10.1016/j.bpc.2008.11.014.

## References

[1] T. Kojaoghlanian, P. Flomenberg, M.S. Horwitz, The impact of adenovirus infection on the immunocompromised host, Rev. Med. Virol. 13 (2003) 155–171.
[2] CDC, Acute respiratory disease associated with adenovirus serotype 14-four states, 2006–2007, MMWR Morb. Mortal. Wkly. Rep. 56 (2007) 1181–1184.
[3] P. Ljungman, Treatment of adenovirus infections in the immunocompromised host, Eur. J. Clin. Microbiol. Infect. Dis. 23 (2004) 583–588.
[4] D. Metzgar, M. Osuna, A.E. Kajon, A.W. Hawksworth, M. Irvine, K.L. Russell, Abrupt emergence of diverse species B adenoviruses at US military recruit training centers, J. Infect. Dis. 196 (2007) 1465–1473.
[5] N.E. Bowles, G.S. Shirali, R.E. Chinnock, G.L. Rosenthal, J.A. Towbin, Association of viral genome with transplant coronary arteriopathy and graft loss in children following cardiac transplantation, J. Heart Lung Transplant. 20 (2001) 198.
[6] G.S. Shirali, J. Ni, R.E. Chinnock, J.K. Johnston, G.L. Rosenthal, N.E. Bowles, J.A. Towbin, Association of viral genome with graft loss in children after cardiac transplantation, N. Engl. J. Med. 344 (2001) 1498–1503.
[7] M.J. McConnell, M.J. Imperiale, Biology of adenovirus and its use as a vector for gene therapy, Hum. Gene Ther. 15 (2004) 1022–1033.
[8] L. Prage, U. Pettersson, Structural proteins of adenoviruses. VII. Purification and properties of an arginine-rich core protein from adenovirus type 2 and type 3, Virology 45 (1971) 364–373.
[9] P. Ostapchuk, P. Hearing, Control of adenovirus packaging, J. Cell. Biochem. 96 (2005) 25–35.
[10] L.W. Black, DNA packaging in dsDNA bacteriophages, Annu. Rev. Microbiol. 43 (1989) 267–292.
[11] C.E. Catalano, The terminase enzyme from bacteriophage lambda: a DNA-packaging machine, Cell. Mol. Life Sci. 57 (2000) 128–148.
[12] B. Sundquist, E. Everitt, L. Philipson, S. Hoglund, Assembly of adenoviruses, J. Virol. 11 (1973) 449–459.
[13] J.C. D'Halluin, M. Milleville, P.A. Boulanger, G.R. Martin, Temperature-sensitive mutant of adenovirus type 2 blocked in virion assembly: accumulation of light intermediate particles, J. Virol. 26 (1978) 344–356.
[14] T.B. Hasson, P.D. Soloway, D.A. Ornelles, W. Doerfler, T. Shenk, Adenovirus L1 52- and 55-kilodalton proteins are required for assembly of virions, J. Virol. 63 (1989) 3612–3621.
[15] P.K. Chatterjee, M.E. Vayda, S.J. Flint, Adenoviral protein VII packages intracellular viral DNA throughout the early phase of infection, Embo. J. 5 (1986) 1633–1644.
[16] P.K. Chatterjee, U.C. Yang, S.J. Flint, Comparison of the interactions of the adenovirus type 2 major core protein and its precursor with DNA, Nucleic Acids Res. 14 (1986) 2721–2735.
[17] C.V. Dery, M. Toth, M. Brown, J. Horvath, S. Allaire, J.M. Weber, The structure of adenovirus chromatin in infected cells, J. Gen. Virol. 66 (Pt 12) (1985) 2671–2684.
[18] J. Weber, L. Philipson, Protein composition of adenovirus nucleoprotein complexes extracted from infected cells, Virology 136 (1984) 321–327.
[19] W. Zhang, R. Arcos, Interaction of the adenovirus major core protein precursor, pVII, with the viral DNA packaging machinery, Virology 334 (2005) 194–202.
[20] J.R. Putnak, B.A. Phillips, Picornaviral structure and assembly, Microbiol. Rev. 45 (1981) 287–315.
[21] B. Rombaut, R. Vrijsen, A. Boeye, New evidence for the precursor role of 14S subunits in poliovirus morphogenesis, Virology 177 (1990) 411–414.
[22] Y. Verlinden, A. Cuconati, E. Wimmer, B. Rombaut, Cell-free synthesis of poliovirus: 14S subunits are the key intermediates in the encapsidation of poliovirus RNA, J. Gen. Virol. 81 (2000) 2751–2754.
[23] W. Zhang, M.J. Imperiale, Requirement of the adenovirus IVa2 protein for virus assembly, J. Virol. 77 (2003) 3586–3594.
[24] C. Tribouley, P. Lutz, A. Staub, C. Kedinger, The product of the adenovirus intermediate gene IVa2 is a transcriptional activator of the major late promoter, J. Virol. 68 (1994) 4450–4457.

[25] P. Lutz, C. Kedinger, Properties of the adenovirus IVa2 gene product, an effector of late-phase-dependent activation of the major late promoter, J. Virol. 70 (1996) 1396–1405.
[26] H. Ali, G. LeRoy, G. Bridge, S.J. Flint, The adenovirus L4 33-kilodalton protein binds to intragenic sequences of the major late promoter required for late phase-specific stimulation of transcription, J. Virol. 81 (2007) 1327–1338.
[27] P. Ostapchuk, J. Yang, E. Auffarth, P. Hearing, Functional interaction of the adenovirus IVa2 protein with adenovirus type 5 packaging sequences, J. Virol. 79 (2005) 2831–2838.
[28] A. Pardo-Mateos, C.S. Young, A 40 kDa isoform of the type 5 adenovirus IVa2 protein is sufficient for virus viability, Virology 324 (2004) 151–164.
[29] S.G. Ewing, S.A. Byrd, J.B. Christensen, R.E. Tyler, M.J. Imperiale, Ternary complex formation on the adenovirus packaging sequence by the IVa2 and L4 22-kilodalton proteins, J. Virol. 81 (2007) 12450–12457.
[30] R.E. Tyler, S.G. Ewing, M.J. Imperiale, Formation of a multiple protein complex on the adenovirus packaging sequence by the IVa2 protein, J. Virol. 81 (2007) 3447–3454.
[31] W. Zhang, M.J. Imperiale, Interaction of the adenovirus IVa2 protein with viral packaging sequences, J. Virol. 74 (2000) 2687–2693.
[32] M. Grable, P. Hearing, Adenovirus type 5 packaging domain is composed of a repeated element that is functionally redundant, J. Virol. 64 (1990) 2047–2056.
[33] S.I. Schmid, P. Hearing, Bipartite structure and functional independence of adenovirus type 5 packaging elements, J. Virol. 71 (1997) 3375–3384.
[34] P. Ostapchuk, M.E. Anderson, S. Chandrasekhar, P. Hearing, The L4 22-kilodalton protein plays a role in packaging of the adenovirus genome, J. Virol. 80 (2006) 6973–6981.
[35] P. Perez-Romero, R.E. Tyler, J.R. Abend, M. Dus, M.J. Imperiale, Analysis of the interaction of the adenovirus L1 52/55-kilodalton and IVa2 proteins with the packaging sequence in vivo and in vitro, J. Virol. 79 (2005) 2366–2374.
[36] S.P. Fessler, C.S. Young, The role of the L4 33K gene in adenovirus infection, Virology 263 (1999) 507–516.
[37] V. Kulshreshtha, L.A. Babiuk, S.K. Tikoo, Role of bovine adenovirus-3 33K protein in viral replication, Virology 323 (2004) 59–69.
[38] J.D. Meyer, A. Hanagan, M.C. Manning, C.E. Catalano, The phage lambda terminase enzyme: 1. reconstitution of the holoenzyme from the individual subunits enhances the thermal stability of the small subunit, Int. J. Biol. Macromol. 23 (1998) 27–36.
[39] S.C. Gill, P.H. von Hippel, Calculation of protein extinction coefficients from amino acid sequence data, Anal. Biochem. 182 (1989) 319–326.
[40] C.R. Cantor, M.M. Warshaw, H. Shapiro, Oligonucleotide interactions. 3. Circular dichroism studies of the conformation of deoxyoligonucleotides, Biopolymers 9 (1970) 1059–1077.
[41] N.K. Maluf, T.M. Lohman, Self-association equilibria of *Escherichia coli* UvrD helicase studied by analytical ultracentrifugation, J. Mol. Biol. 325 (2003) 889–912.
[42] P. Schuck, On the analysis of protein self-association by sedimentation velocity analytical ultracentrifugation, Anal Biochem 320 (2003) 104–124.
[43] T.M. Laue, B.D. Shah, T.M. Ridgeway, S.L. Pelletier, Analytical Ultracentrifugation in Biochemistry and Polymer Science, Royal Society of Chemistry, Cambridge [England], 1992, p. xiii, 629 pp.
[44] I.D. Kuntz, Hydration of macromolecules. IV. Polypeptide conformation in frozen solutions, J. Am. Chem. Soc. 93 (1971) 516–518.
[45] V.N. Uversky, What does it mean to be natively unfolded? Eur J Biochem 269 (2002) 2–12.
[46] G.H. Koenderink, K.L. Planken, R. Roozendaal, A.P. Philipse, Monodisperse DNA restriction fragments II. Sedimentation velocity and equilibrium experiments, J. Colloid Interface Sci. 291 (2005) 126–134.
[47] R.T. Kovacic, K.E. van Holde, Sedimentation of homogeneous double-strand DNA molecules, Biochemistry 16 (1977) 1490–1498.
[48] G.F. Bonifacio, T. Brown, G.L. Conn, A.N. Lane, Comparison of the electrophoretic and hydrodynamic properties of DNA and RNA oligonucleotide duplexes, Biophys. J. 73 (1997) 1532–1538.
[49] C.R. Cantor, P.R. Schimmel, Biophysical chemistry, vol. II, W. H. Freeman, San Francisco, 1980.
[50] H. Durchschlag, P. Zipper, Comparative investigations of biopolymer hydration by physicochemical and modeling techniques, Biophys. Chem. 93 (2001) 141–157.
[51] R.M. Litman, A deoxyribonucleic acid polymerase from *Micrococcus luteus* (*Micrococcus lysodeikticus*) isolated on deoxyribonucleic acid-cellulose, J. Biol. Chem. 243 (1968) 6222–6233.
[52] J.J. Correia, Analysis of weight average sedimentation velocity data, Methods Enzymol. 321 (2000) 81–100.
[53] W.F. Stafford III, Boundary analysis in sedimentation velocity experiments, Methods Enzymol. 240 (1994) 478–501.
[54] M.J. Jezewska, W. Bujalowski, A general method of analysis of ligand binding to competing macromolecules using the spectroscopic signal originating from a reference macromolecule. Application to *Escherichia coli* replicative helicase DnaB protein nucleic acid interactions, Biochemistry 35 (1996) 2117–2128.
[55] W. Zhang, J.A. Low, J.B. Christensen, M.J. Imperiale, Role for the adenovirus IVa2 protein in packaging of viral DNA, J. Virol. 75 (2001) 10446–10454.
[56] D.F. Senear, R. Batey, Comparison of operator-specific and nonspecific DNA binding of the lambda cI repressor: [KCl] and pH effects, Biochemistry 30 (1991) 6677–6688.
[57] J.A. Holbrook, O.V. Tsodikov, R.M. Saecker, M.T. Record Jr., Specific and non-specific interactions of integration host factor with DNA: thermodynamic evidence for disruption of multiple IHF surface salt-bridges coupled to DNA binding, J. Mol. Biol. 310 (2001) 379–401.